

Supporting Information

Plasticization of poly(3-hydroxybutyrate-co-3-hydroxyvalerate) with an oligomeric polyester: Miscibility and effect of the microstructure and plasticizer distribution on the thermal and mechanical properties.

*Jacqueline L. Barbosa, Giovanni B. Perin, Maria Isabel Felisberti**

Institute of Chemistry, University of Campinas, P.O. BOX: 6154, 13083-970, Campinas
- SP, Brazil

Table of contents

Section	Page
1. Thermogravimetric curves and their derivative curves	S2
2. Deconvolution of DMA curves	S3
3. Estimation of the PLAP composition in amorphous phases	S5
4. SAXS analysis	S7
5. Digital images of the spherulites	S10
6. Determination of the Flory-Huggins interaction parameter	S11
7. Mechanical properties	S13
8. Efficiency of plasticizers – a short review	S14
9. ¹ H and ¹³ C NMR spectra of PHBV	S19
10. ¹ H and ¹³ C NMR spectra of PLAP	S20

1. Thermogravimetric curves and their derivative curves

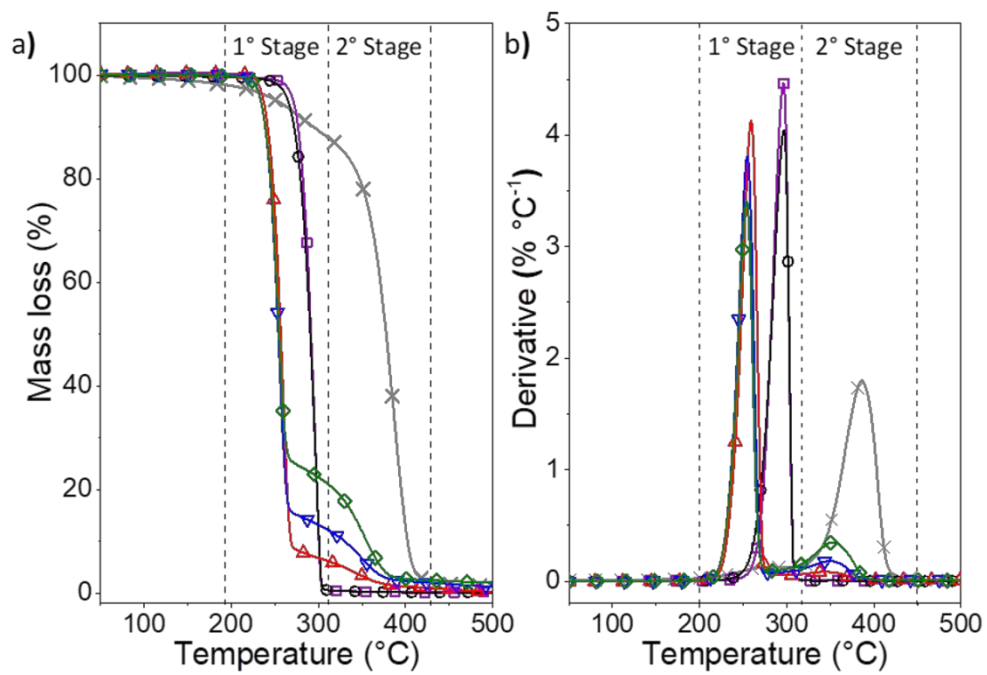


Figure S1: a) TGA curves and b) derivative curves for unprocessed PHBV (□) and PLAP (x), and for the processed PHBV (o) and its formulations with PLAP mass fractions of 0.1 (△), 0.2 (▽) and 0.3 (◇).

2. Deconvolution of DMA curves

The E'' vs T curves deconvoluted by Gaussian curves are presented in Figure S2.

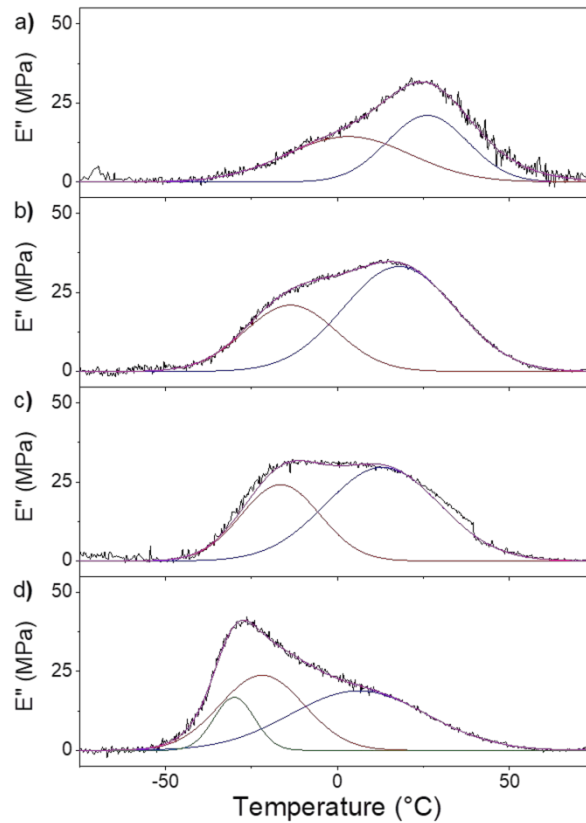


Figure S2: E'' vs T curves (black line) and their Gaussians for a) pure PHBV and its formulations with PLAP mass fractions of b) 0.1, c) 0.2, and d) 0.3.

The deconvolution of the $\tan \delta$ vs T and E'' vs T curves using Gaussians allows for the determination of the T_g of the rigid and mobile amorphous phases as the temperatures corresponding to the maximums of the Gaussians, which are summarized in Table S1 and S2.

Table S1: T_g and PHB and PLAP mass fraction in the rigid, mobile, and PLA-rich mobile amorphous phases determined from the deconvoluted $\tan \delta$ vs T curves for PHBV and its formulations with PLAP mass fractions of 0.1, 0.2, and 0.3.

w_{PLAP}	Rigid amorphous phase			Mobile amorphous phase			PLAP-rich mobile amorphous phase		
	T_g (°C)	w_{PHBV}	w_{PLAP}	T_g (°C)	w_{PHBV}	w_{PLAP}	T_g (°C)	w_{PHBV}	w_{PLAP}
0.0	28	1.00	0.00	3	1.00	0.00	---	---	---
0.1	24	0.94	0.06	-8	0.71	0.29	---	---	---
0.2	22	0.91	0.09	-10	0.66	0.34	---	---	---
0.3	12	0.77	0.23	-10	0.64	0.36	-27.0	0.13	0.87

Table S2: T_g and PHB and PLAP mass fraction in the rigid, mobile and PLA-rich mobile amorphous phases determined from the deconvoluted E'' vs T curves for PHBV and its formulations with PLAP mass fractions of 0.1, 0.2, and 0.3.

w_{PLAP}	Rigid amorphous phase			Mobile amorphous phase			PLAP-rich mobile amorphous phase		
	T_g (°C)	w_{PHBV}	w_{PLAP}	T_g (°C)	w_{PHBV}	w_{PLAP}	T_g (°C)	w_{PHBV}	w_{PLAP}
0.0	26	1.00	0.00	3	1.00	0.00	---	---	---
0.1	18	0.88	0.12	-14	0.53	0.47	---	---	---
0.2	13	0.80	0.20	-16	0.46	0.54	---	---	---
0.3	6	0.70	0.30	-22	0.30	0.70	-30	0.04	0.96

3. Estimation of the PLAP composition in amorphous phases

The PLAP mass fractions in the mobile and rigid amorphous phases were graphically estimated from the T_g of the mobile and rigid amorphous phases for pure PHBV (determined from $\tan \delta$ vs T and E'' vs T curves) and for PLAP (determined by DSC). The composition-dependence of the T_g of the mobile and rigid amorphous phases were plotted by using the Fox equation⁷⁶ (Equation S1), assuming that it adequately describes the dependence of T_g on the formulations composition, and presented in Figure S3.

$$\frac{1}{T_g} = \frac{w_{PHBV}}{T_{g,PHBV}} + \frac{(1-w_{PHBV})}{T_{g,PLAP}} \quad \text{Equation S1}$$

where $T_{g,PHBV}$, $T_{g,PLAP}$, and T_g are the glass transition temperatures of the pure PHBV, pure PLAP, and of the mobile or rigid amorphous phase, respectively.

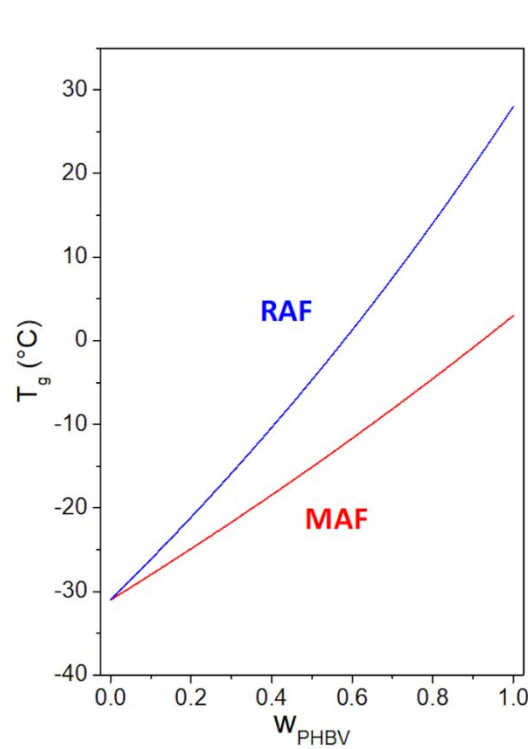


Figure S3: T_g of the mobile (-) and rigid (-) amorphous phases as a function of the PHBV mass fraction in the formulations with PLAP predicted by the Fox equation.

The compositions of each amorphous phase in the PHBV formulations (determined from $\tan \delta$ vs T and E'' vs T curves) are presented in Tables S1 and S2, respectively. The T_g of each phase and the PHBV and PLAP mass fraction (w_i) in each phase (i) for pure PHBV and its plasticized formulations (determined using data from E'' vs T curves) are presented in Figure 4S.

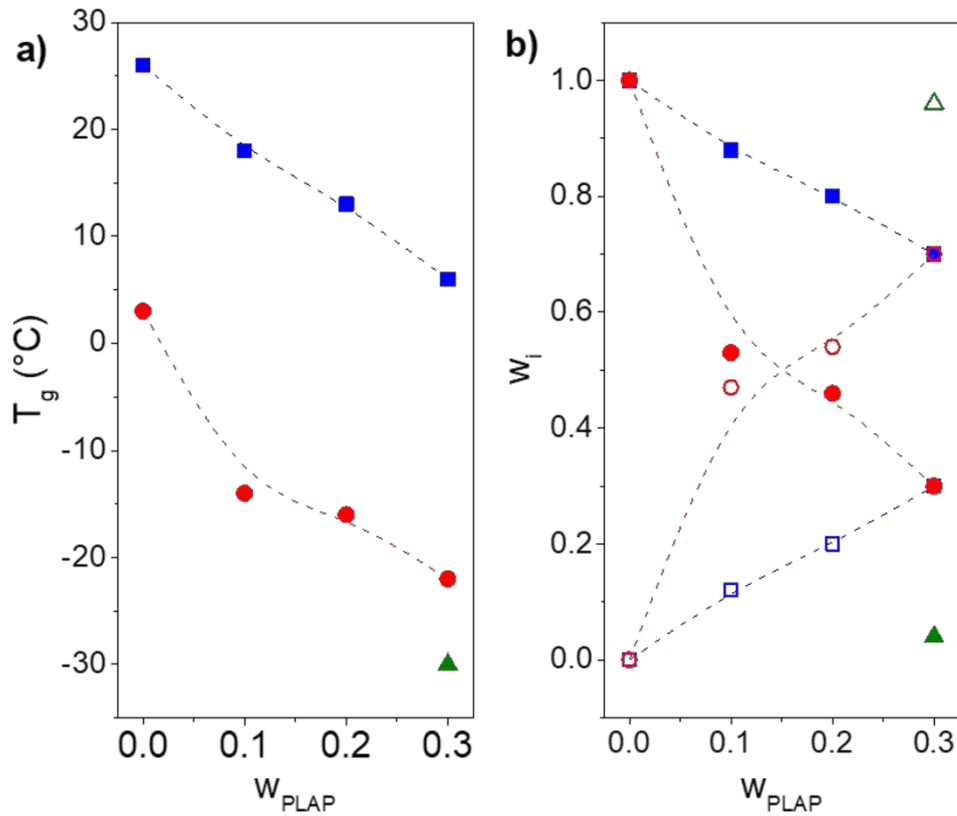


Figure S4: a) T_g and b) the PHBV (closed symbols) and PLAP (open symbols) mass fraction in the amorphous phases as a function of the PLAP mass fraction in the formulations: rigid (■, □), mobile (●, ○), and PLAP-rich mobile amorphous phases (▲, △). Data determined from E'' vs T curves.

4. SAXS analysis

The Lorentz corrected SAXS for aged and recrystallized samples of processed PHBV and its formulations with PLAP are presented in Figure S5.

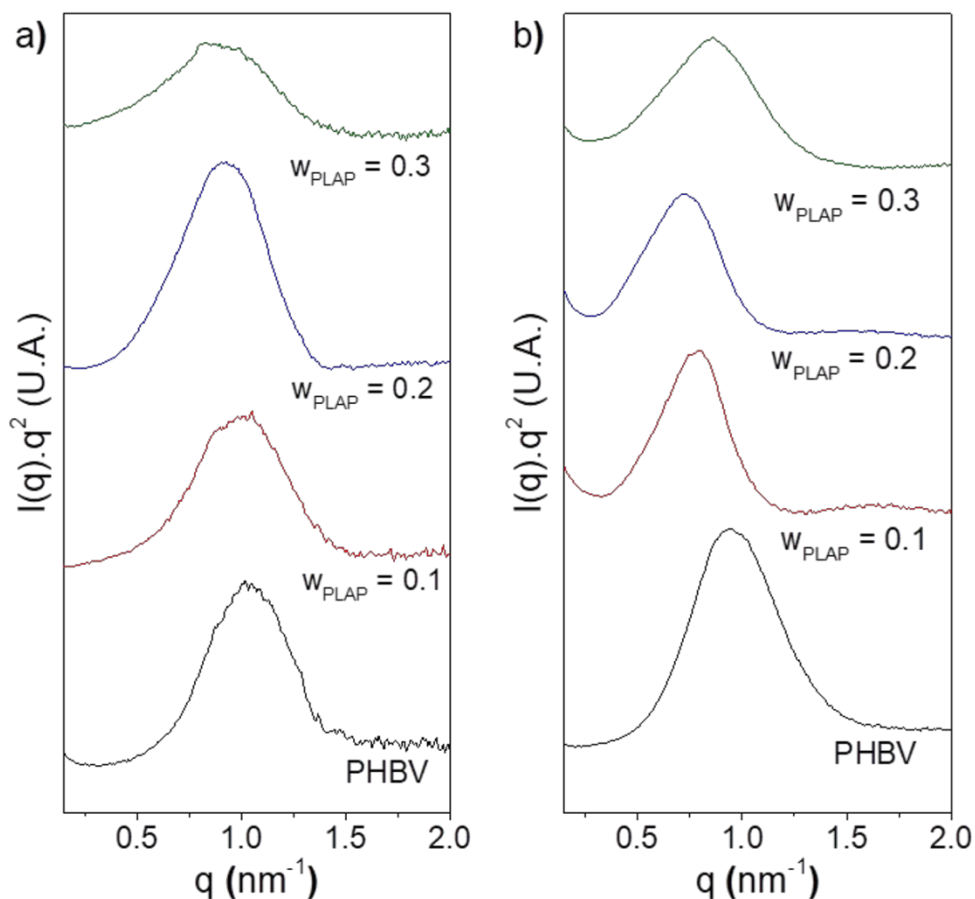


Figure S5: Lorentz-corrected $I(q)q^2$ vs q curves for a) aged and b) recrystallized PHBV (-) and its formulations with PLAP mass fractions of 0.1 (-), 0.2 (-), and 0.3 (-).

The long period (L_p), the crystalline lamella (l_c), and the amorphous layer (l_a) were determined by using SAXDAT software. Based on the lamellar stack model of the polymer structure the morphological parameters were calculated using a correlation function as an inverse Fourier transform of the intensity distribution function.⁷³ From the correlation function, the thickness of the two phases (crystalline and amorphous) was determined, and the attribution of each phase was performed by comparing the volumetric degree of crystallinity of the formulation (Φ_c , equation S2) with the linear degree of crystallinity within the lamellar stacks (ϕ_c^{lin} , equation S3):⁷⁴

$$\Phi_c = \frac{\chi_c / \rho_c}{\chi_c / \rho_c - PHBV + \frac{(w_{PHB} - \chi_c)}{\rho_a} + \frac{w_{PLAP}}{\rho_{PLAP}}} \quad \text{Equation S2}$$

where χ_c is the degree of crystallinity measured by DSC, ρ_c and ρ_a are the densities of 100% crystalline PHB ($\rho_c = 1.26 \text{ g cm}^{-3}$) and completely amorphous PHB ($\rho_c = 1.18 \text{ g cm}^{-3}$)⁴, ρ_{PLAP} is the PLAP density ($\rho_{PLAP} = 1.18 \text{ g cm}^{-3}$, determined by using a pycnometer), and w_{PHBV} and w_{PLAP} are the PHBV and PLAP mass fraction in the formulations.

$$\phi_c^{lin} = l_c / L_p \quad \text{Equation S3}$$

The correlation functions for aged and recrystallized samples for processed PHBV and its formulations with PLAP are presented in Figure S6.

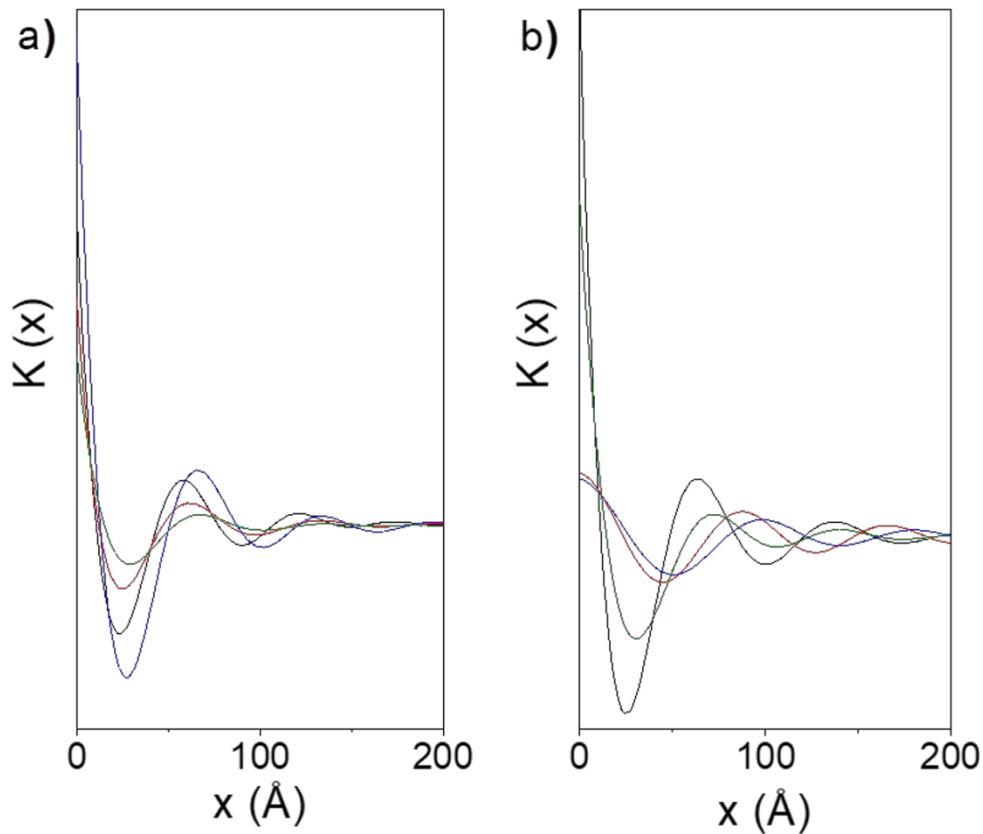


Figure S6: Correlation functions for a) aged and b) recrystallized samples for processed PHBV (-) and its formulations with PLAP mass fractions of 0.1 (-), 0.2 (-), and 0.3 (-).

The structural parameters determined by SAXS are summarized in Table S3.

Table S3: Scattering vector at the peak maximum (q_{\max}), long period (L_p), crystalline lamellae and amorphous layers thickness (l_c and l_a , respectively), linear degree of crystallinity within the lamellar stacks (ϕ_c^{lin}), and the volumetric degree of crystallinity (Φ_c) for aged specimens and thin films freshly crystallized at 70°C for 1 h.

Aged specimens							Films freshly crystallized at 70°C for 1 h					
w_{PLAP}	q_{\max} (nm^{-1})	L_p (nm)	l_c (nm)	l_a (nm)	Φ_c	ϕ_c^{lin}	q_{\max} (nm^{-1})	L_p (nm)	l_c (nm)	l_a (nm)	Φ_c	ϕ_c^{lin}
0.0	1.03	5.8	4.4	1.4	0.53	0.76	0.94	6.2	4.7	1.5	0.56	0.76
0.1	0.99	6.1	4.7	1.4	0.55	0.77	0.78	8.7	5.1	3.6	0.51	0.58
0.2	0.92	6.5	4.8	1.7	0.56	0.75	0.72	9.8	5.7	4.1	0.46	0.58
0.3	0.89	6.7	4.9	1.8	0.60	0.72	0.86	7.3	5.4	1.9	0.41	0.75

5. Digital images of the spherulites

Digital images of unprocessed PHBV, processed PHBV, and its formulations with PLAP isothermally crystallized at 55, 65, and 75 °C are presented in Figure S7.

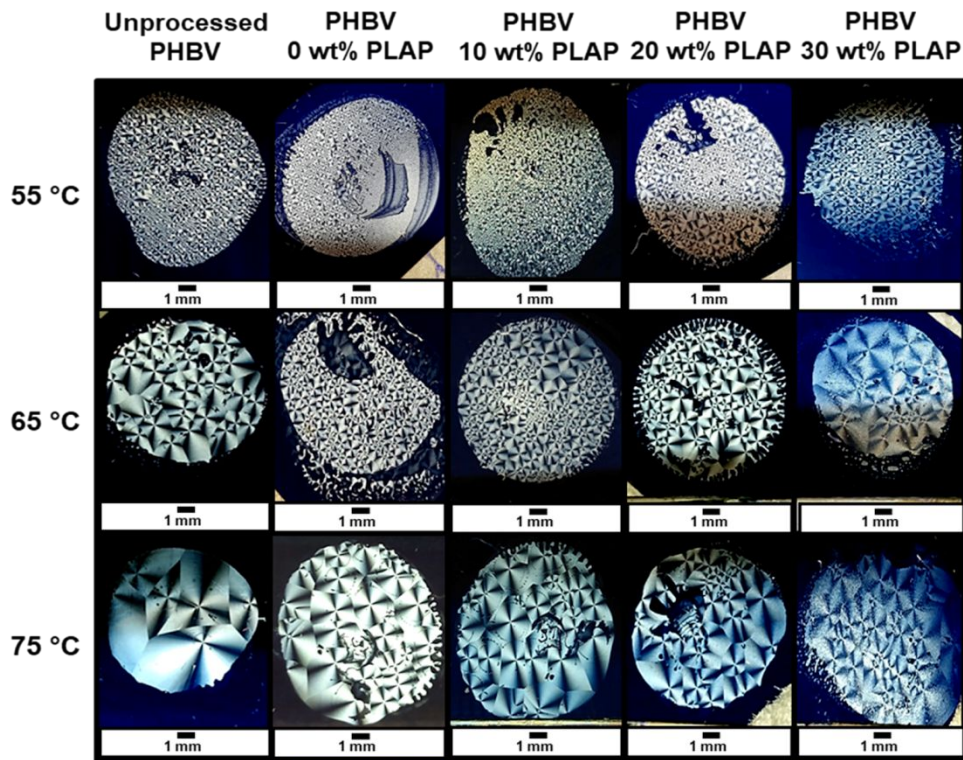


Figure S7: Digital images of unprocessed PHBV, processed PHBV, and its formulations with PLAP isothermally crystallized at 55, 65, and 75 °C.

6. Determination of the Flory-Huggins interaction parameter

The depression in the melting point of the plasticized PHBV was investigated according to the Flory-Huggins theory and the Nishi-Wang equation⁶⁸ (Equation 4):

$$\left(\frac{1}{T'_m} - \frac{1}{T_m^o}\right) = - \left(\frac{RV_{2u}}{\Delta H_{2u}V_{1u}}\right) * \left[\left(\frac{\ln\phi_2}{Dp_2}\right) + \left(\frac{1}{Dp_2} - \frac{1}{Dp_1}\right)\phi_1 + \chi_{12}\phi_1^2\right] \text{ Equation S4}$$

where, T'_m and T_m^o are the melting temperatures of the plasticized and pure PHBV, respectively. Subscript 1 denotes the plasticizer PLAP and subscript 2 the PHBV. V_u is the molar volume of the mers, ΔH_u is the enthalpy of melting per mole of mers, Dp is the degree of polymerization, R is the universal gas constant, ϕ is the volume fraction, and $\chi_{1,2}$ is the Flory-Huggins interaction parameter. Rearranging equation S4 gives the following:

$$- \left[\left(\frac{\Delta H_{2u}V_{1u}}{RV_{2u}}\right)\left(\frac{1}{T'_m} - \frac{1}{T_m^o}\right)\right] - \left(\frac{\ln\phi_2}{Dp_2}\right) - \left(\frac{1}{Dp_2} - \frac{1}{Dp_1}\right)\phi_1 = \beta = \chi_{1,2}\phi_1^2 \quad \text{Equation S5}$$

$\chi_{1,2}$ is the slope of the curve of β as a function of ϕ_1^2 (Figure S8).

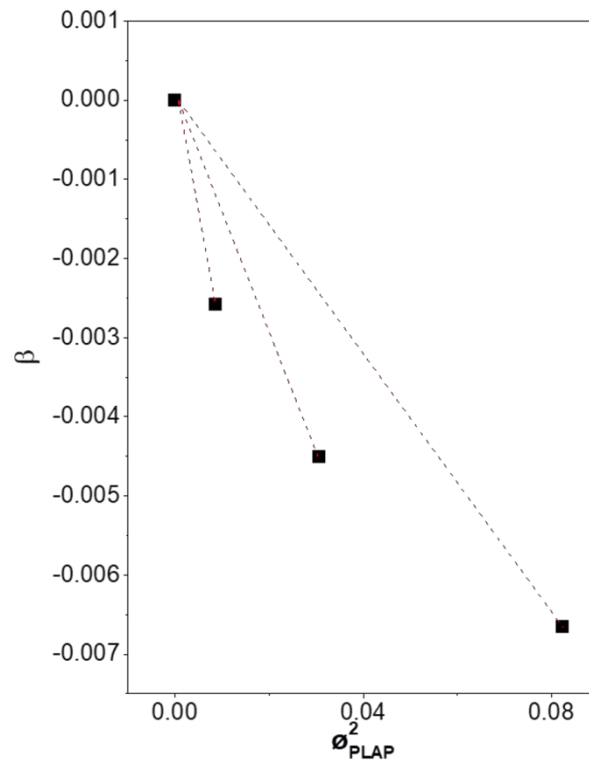


Figure S8: Plot of β vs ϕ^2_{PLAP} according to Equation S5.

7. Mechanical properties

Table S4 summarizes the results from the Izod impact resistance and tensile test analysis.

Table S4: Izod impact resistance, elastic modulus, tensile strength, and elongation at break for the specimens of PHBV and its formulations with PLAP mass fractions of 0.1, 0.2, and 0.3.

W_{PLAP}	Izod Impact Resistance (J m^{-1})	Elastic Modulus (MPa)	Tensile Strength (MPa)	Strain at Break (%)
0.0	96 ± 10	586 ± 28	30.5 ± 1.4	8.0 ± 0.0
0.1	130 ± 20	502 ± 16	26.3 ± 0.3	8.2 ± 0.4
0.2	224 ± 60	428 ± 35	22.2 ± 1.2	8.1 ± 0.4
0.3	212 ± 40	381 ± 22	18.9 ± 0.4	6.6 ± 0.5

10. Efficiency of plasticizers – a short review

To compare our data with data from literature for low molar mass and oligomeric plasticizers for PHB and PHBV, we choose the following parameters:

1. Depression of T_g expressed as

$$\Delta T_g = T_{g(\text{Formulation})} - T_{g(\text{Matrix})} \text{ (}^\circ\text{C)} \quad \text{Equation S6}$$

2. Depression of T_m expressed as

$$\Delta T_m = T_{m(\text{Formulation})} - T_{m(\text{Matrix})} \text{ (}^\circ\text{C)} \quad \text{Equation S7}$$

3. Percent change in the elastic modulus, E , expressed as

$$\Delta E = \left(\frac{E_{(\text{Formulation})} - E_{(\text{Matrix})}}{E_{(\text{Matrix})}} \right) \times 100 \quad \text{Equation S8}$$

4. Percent change in the elongation at break, ε , expressed as

$$\Delta \varepsilon = \varepsilon_{\text{Formulation}} - \varepsilon_{\text{Matrix}} \quad \text{Equation S9}$$

These data for oligomeric and molecular plasticized PHB and PHBV are compiled in Tables S5 and S6, respectively.

Table S5: Efficiency of oligomeric plasticizers for decreasing T_g and T_m and for tuning the mechanical properties of the PHB and PHBV formulations.

Matrix	Plasticizer	Mass fraction	ΔT_g (°C)	ΔT_m (°C)	ΔE (%)	$\Delta \varepsilon$ (%)	Reference
PHBV (3% HV, $M_w = 250$ kDa)	PLAP ($M_w = 6.5$ kDa)	0.1	-3	-1	-14	0.2	this work
PHBV (3% HV, $M_w = 250$ kDa)	PLAP ($M_w = 6.5$ kDa)	0.2	-6	-2	-27	0.1	this work
PHBV (3% HV, $M_w = 250$ kDa)	PLAP ($M_w = 6.5$ kDa)	0.3	-11	-3	-35	-1.4	this work
PHBV (3% HV, $M_w = 250$ kDa)	PEG1000	0.1	n.d.	-1	-37	0.8	24
PHBV (3% HV, $M_w = 250$ kDa)	PEG1000	0.2	n.d.	0	-28	0.2	24
PHB	Poly(adipate) ($M_n = 3.8$ kDa)	0.1	-9	-4	-25	-0.2	32
PHB	Poly(adipate) ($M_n = 3.8$ kDa)	0.2	-17	-5	-43	1.8	32
PHB	Poly(adipate) ($M_n = 3.8$ kDa)	0.3	-32	-7	-53	3.5	32
PHBV (8% HV)	PEG200	0.1	0,0	-5	-14	0.4	39
PHBV (8% HV)	PEG1000	0.1	0,0	-2	-31	0.8	39
PHBV (8% HV)	PEG4000	0.1	0,0	-2	-30	0.3	39
PHBV (3% HV)	PEG400	0.1	-15	-6	-56	4.0	45
PHBV (3% HV)	PEG1000	0.1	n.d.	-4	-37	2.7	45
PHBV (3% HV)	PEG4000	0.1	n.d.	-2	-48	2.8	45
PHB ($M_w = 600$ kDa)	Poly[di(ethyleneglycol) adipate] ($M_n = 2.5$ kDa)	0.1	-10	-1	0	0.0	46
PHB ($M_w = 600$ kDa)	Poly[di(ethyleneglycol) adipate] ($M_n = 2.5$ kDa)	0.2	-13	-2	-25	0.0	46
PHB ($M_w = 600$ kDa)	Poly[di(ethyleneglycol) adipate] ($M_n = 2.5$ kDa)	0.3	-15	-2	-28	1.0	46
PHB	PEG4000	0.1	n.d.	-5	-36	-0.2	47
PHB	PEG6000	0.1	n.d.	-3	-27	0.7	47
PHB ($M_n = 190$ kDa)	PEG300	0.1	-15	-3	n.d.	7.0	49
PHB ($M_n = 190$ kDa)	Laprol 503	0.1	-13	-1	n.d.	7.0	49
PHB ($M_n = 190$ kDa)	Laprol 5003 ($M_n = 5.0$ kDa)	0.1	-1	2	n.d.	7.0	49
PHB ($M_n = 190$ kDa)	PHB ($M_w = 3.6$ kDa)	0.1	n.d.	0	-22	-0.9	63
PHB ($M_n = 190$ kDa)	PHB ($M_w = 3.6$ kDa)	0.2	n.d.	0	-12	-3.3	63
PHB ($M_n = 190$ kDa)	PHB-diol ($M_w = 1.8$ kDa)	0.2	-12	-11	n.d.	3.0	64
PHB	atactic PHB ($M_n = 0.6$ kDa)	0.1	-30	-4	n.d.	n.d.	65
PHB	atactic PHB ($M_n = 0.6$ kDa)	0.3	-52	-8	n.d.	n.d.	65
PHB	atactic PHB ($M_n = 2.7$ kDa)	0.1	-18	-2	n.d.	n.d.	65
PHB	atactic PHB ($M_n = 2.7$ kDa)	0.3	-23	-6	n.d.	n.d.	65
PHB	medium-chain-length PHA ($M_n = 4.6$ kDa)	0.1	n.d.	-0,9	-38	-5.0	66
PHB	medium-chain-length PHA ($M_n = 4.6$ kDa)	0.2	n.d.	-7,6	-62	2.0	66

Continuation of Table S5.

Matrix	Plasticizer	Mass fraction	ΔT_g (°C)	ΔT_m (°C)	ΔE (%)	$\Delta \epsilon$ (%)	Reference
PHB ($M_w = 370$ kDa)	Pluronic F68 ($M_w = 8.4$ kDa)	0.2	-10	-2	20	-12,6	67
PHB ($M_w = 370$ kDa)	Pluronic F127 ($M_w = 12.6$ kDa)	0.2	-10	-3	n.d.	n.d.	67
PHBV (5% HV, $M_n = 300$ kDa)	Poly(caprolactone)-triol	0.1	-11	-2	n.d.	n.d.	69
PHBV (5% HV, $M_n = 300$ kDa)	Poly(caprolactone)-triol	0.2	-12	-6	n.d.	n.d.	69
PHBV (5% HV, $M_n = 300$ kDa)	Poly(caprolactone)-triol	0.3	-12	-8	n.d.	n.d.	69
PHB (ENMAT Y1000)	Tolonate X FLO100	0.1	n.d.	0	-1	2.0	70
PHB (ENMAT Y1000)	Tolonate X FLO100	0.2	n.d.	-1	-20	4.0	70

n.d. – not determined.

Table S6: Efficiency of low molar mass plasticizers for decreasing T_g and T_m and for tuning the mechanical properties of PHB and PHBV.

Matrix	Plasticizer	Mass fraction	ΔT_g (°C)	ΔT_m (°C)	ΔE (%)	$\Delta \epsilon$ (%)	Reference
PHB ($M_n = 330$ kDa)	Diethyl sebacate	0.3	-10	-5	-75	1,8	31
PHB ($M_n = 330$ kDa)	Acetyl tributyl citrate	0.1	-16	-6	-9	3,6	31
PHB ($M_n = 330$ kDa)	Acetyl tributyl citrate	0.2	-35	-9	-55	6,0	31
PHB ($M_n = 330$ kDa)	Acetyl tributyl citrate	0.3	-37	-12	-87	7,2	31
PHB	Diethyl phthalate	0.1	-9,5	-5	-39	3,5	32
PHB	Diethyl phthalate	0.2	-10,1	-6	-51	3,1	32
PHB	Diethyl phthalate	0.3	-11,5	-9	-63	1,6	32
PHB	Diethyl adipate	0.1	-7,7	-3	-18	-1,3	32
PHB	Diethyl adipate	0.2	-7,6	-6	-37	-0,8	32
PHB	Diethyl adipate	0.3	-7,5	-6	-39	-2,7	32
PHB	Triacetyl glycerol	0.1	-10,4	-6	-43	0,4	32
PHB	Triacetyl glycerol	0.2	-17,4	-11	-74	3,3	32
PHB ($M_w = 800$ kDa)	Salicylic acid decyl ester	0.3	-38	n.d.	-72	102,0	35
PHB ($M_w = 800$ kDa)	Salicylic acid 2-butyloctyl ester	0.3	-38	n.d.	-73	20,0	35
PHB ($M_w = 800$ kDa)	Acetylsalicylic acid hexyl ester	0.3	-24	n.d.	-77	124,0	35
PHB ($M_w = 800$ kDa)	Acetylsalicylic acid dextyl ester	0.3	-17	n.d.	-72	32,0	35
PHB ($M_w = 800$ kDa)	Ketoprofen ethyl ester	0.3	-24	n.d.	-80	56,0	35
PHB ($M_w = 800$ kDa)	Triethyl citrate	0.3	-34	n.d.	-68	19,0	35
PHB ($M_w = 800$ kDa)	Butyryltriethyl citrate	0.3	-33	n.d.	-73	30,0	35
PHBV (8% HV)	Lauric acid	0.1	0	-5	-11	0,1	39
PHBV (8% HV)	Stearic acid	0.1	0	-8	-22	-0,7	39
PHB ($M_w = 670$ kDa)	Glycerol triacetate	0.2	-23,5	-13,2	-58	59	43
PHB ($M_w = 670$ kDa)	Glycerol tripropionate	0.2	-30,3	-12,8	-41	5	43
PHB ($M_w = 670$ kDa)	Glycerol tributyrate	0.2	-30,8	-12,1	-61	21	43
PHB ($M_w = 670$ kDa)	Glycerol tricaproate	0.2	-20,6	-6,3	-49	17	43
PHB ($M_w = 670$ kDa)	Glycerol tricaprilate	0.2	-16,3	-4,2	-53	32	43
PHB ($M_w = 670$ kDa)	Glycerol trilaurate	0.2	-2,4	-0,2	-60	4	43
PHB ($M_w = 670$ kDa)	Glycerol tripalmitate	0.2	-1,4	-1,1	-34	-1	43
PHB ($M_w = 670$ kDa)	Glycerol tristearate	0.2	-3,2	-0,3	-18	-3	43
PHB ($M_w = 670$ kDa)	Glycerol diacetate	0.2	-25,9	-11,2	-23	14	43
PHB ($M_w = 670$ kDa)	Glycerol dilaurate	0.2	-18,7	-5,7	-21	-2	43
PHB ($M_w = 670$ kDa)	Glycerol monoacetate	0.2	-1,8	-11,9	-26	-3	43
PHB ($M_w = 670$ kDa)	Glycerol monolaurate	0.2	-6,6	-12,9	-53	0	43
PHB ($M_w = 670$ kDa)	Glycerol monostearate	0.2	-23,6	-14,7	-49	15	43

Continuation of Table S6.

Matrix	Plasticizer	Mass fraction	ΔT_g (°C)	ΔT_m (°C)	ΔE (%)	$\Delta \varepsilon$ (%)	Reference
PHB ($M_w = 600$ kDa)	Glyceryl tributyrate	0.1	-5	-1	0	1,0	46
PHB ($M_w = 600$ kDa)	Glyceryl tributyrate	0.2	-5	0	-13	2,0	46
PHB ($M_w = 600$ kDa)	Glyceryl tributyrate	0.3	-10	-2	-16	6,0	46
PHB	Acetyl tributyl citrate	0.1	n.d.	-6	-36	2,2	47
PHB	Epoxidized soybean oil	0.1	n.d.	-4	-23	1,8	47
PHB ($M_n = 190$ kDa)	Dibutyl sebacate	0.1	-13	-5	n.d.	7,0	49
PHB ($M_n = 190$ kDa)	Diethyl sebacate	0.1	-5	-2	n.d.	7,0	49
PHB ($M_n = 460$ kDa)	Maleinized linseed oil	0.1	-1,4	-3,8	-15	0,8	52
PHB ($M_n = 460$ kDa)	Maleinized linseed oil	0.2	-1,2	-4,6	-17	-1,5	52
PHB ($M_n = 460$ kDa)	Octyl epoxy stearate	0.1	0,5	-3,4	-23	3,1	52
PHB ($M_n = 460$ kDa)	Octyl epoxy stearate	0.2	0,5	-3,9	-23	1,8	52
PHBV (6% HV)	Soybean oil	0.1	1	-3	-22	-1	54
PHBV (6% HV)	Soybean oil	0.2	2	1	-18	-1,9	54
PHBV (6% HV)	Soybean oil	0.3	3	-2	-20	-2,4	54
PHBV (6% HV)	Epoxidized soybean oil	0.1	-2	-1	-33	1,6	54
PHBV (6% HV)	Epoxidized soybean oil	0.2	-12	-1	-43	1,9	54
PHBV (6% HV)	Epoxidized soybean oil	0.3	-14	-1	-56	2,2	54
PHB	Geraniol	0.1	-13	-7	-42	2,9	57
PHB	Geraniol	0.2	-20	-8	-62	3,1	57
PHB	Linalool	0.1	-11	-6	-44	3,0	57
PHB	Linalool	0.2	-18	-3	-48	3,8	57
PHB	Geraniol acetate	0.1	-17	-6	-52	5,3	57
PHB	Geraniol acetate	0.2	-22	-12	-73	11,7	57
PHB ($M_w = 397$ kDa)	Triethyl citrate	0.1	-10	-6	-20	-0,2	75
PHB ($M_w = 397$ kDa)	Triethyl citrate	0.2	-25	-10	-44	1,6	75
PHB ($M_w = 397$ kDa)	Triethyl citrate	0.3	-29	-18	-63	1,1	75

n.d. – not determined.

8. ^1H and ^{13}C NMR spectra of PHBV

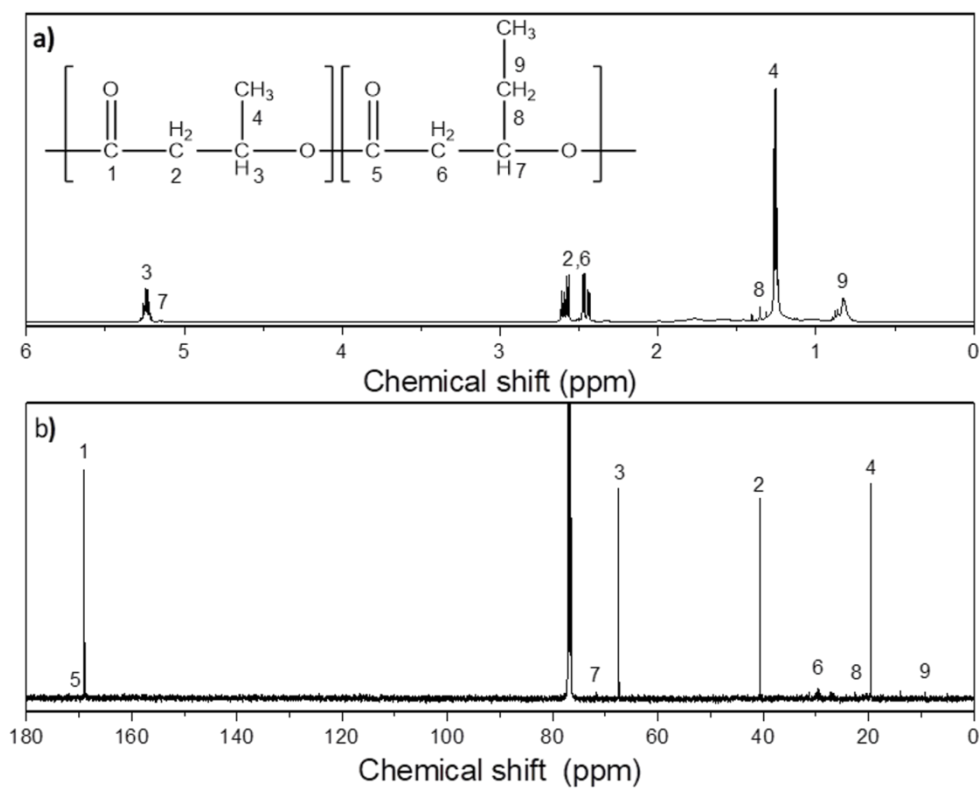


Figure S9: a) ^1H and b) ^{13}C NMR spectra of pure PHBV in CDCl_3 .

9. ^1H and ^{13}C NMR spectra of PLAP

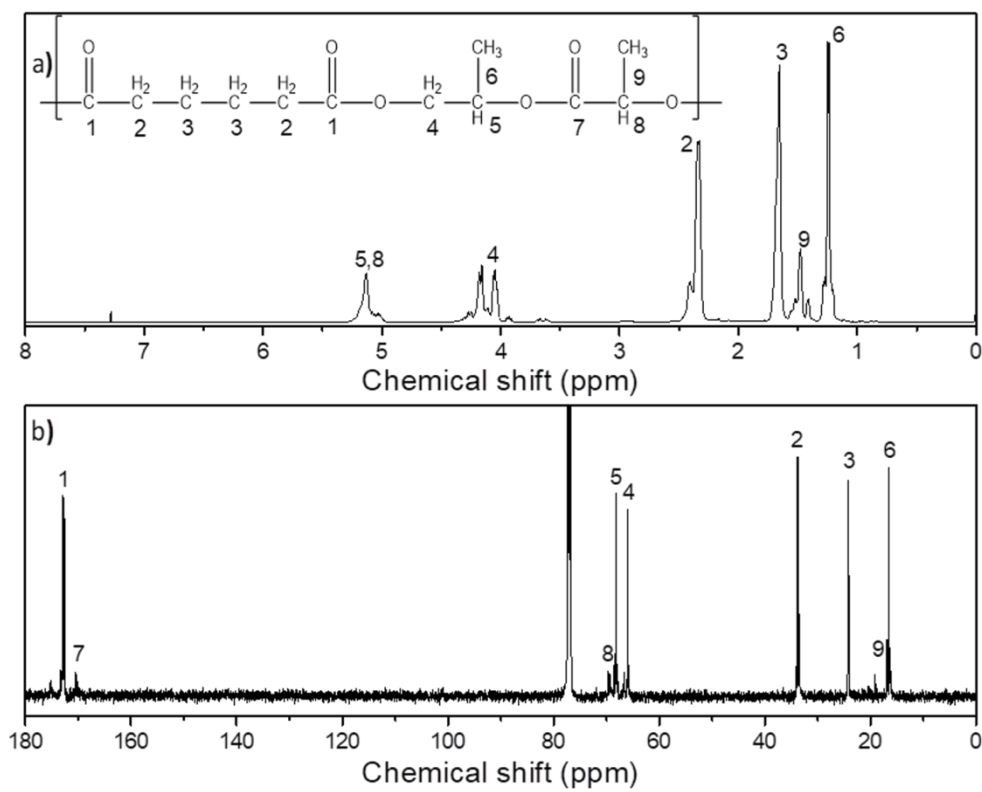


Figure S10: a) ^1H and b) ^{13}C NMR spectra of pure PLAP in CDCl_3 .